EXTREME SOLAR SYSTEMS
ASP Conference Series, Vol. 398, 2008
D. Fischer, F. A. Rasio, S. E. Thorsett, and A. Wolszczan

Dynamically Unstable Planetary Systems Emerging Out of Gas Disks

Soko Matsumura, Edward W. Thommes, Sourav Chatterjee, and Frederic A. Rasio

Northwestern University, Department of Physics and Astronomy, 2131 Tech Drive, Evanston, IL 60208 USA

Abstract. One of the most surprising properties of extrasolar planets is the eccentricity of their orbits, which vary from nearly circular ($e \sim 0$) to highly eccentric ones (up to $e \sim 0.9$). Planet-planet scattering with no gas disk has successfully reproduced the observed eccentricity distribution. However, this scenario alone cannot explain the distribution of planetary semi-major axes if giant planets form outside of $\sim$ 1 AU. Taking into account the effects of a residual gas disk after planet formation, we investigate the onset of dynamical instability in young planetary systems. Using a hybrid symplectic integrator + gas dynamics code, we demonstrate how planet-disk interactions along with planet-planet dynamical interactions could explain both the observed semi-major axis and eccentricity distributions of extrasolar planets.

1. Introduction

The discovery of extrasolar systems have revealed many new features of planets. Some of the most astonishing findings include that a giant planet can orbit extremely close to the central star (down to ~ 2 Roche limit), and that planets can take a wide range of eccentricity (from almost 0 to 0.9). Explaining such features is important to understanding the formation and evolution history of extrasolar planetary systems, which will in turn help us understand our own solar system.

Our goal is to explore a scenario which explains both the semi-major axis and eccentricity distributions of planetary systems self-consistently. The origin of small orbital radii of observed extrasolar planets is usually explained by planet migration due to planet-disk interaction (e.g., Goldreich & Tremaine 1979; Ward 1997), while that of various eccentricities is explained either by planet-disk interaction (e.g., Artymowicz 1993; Goldreich & Sari 2003), planet-planet interaction (e.g., Rasio et al. 1996; Weidenschilling & Marzari 1996; Lin & Ida 1997), or Kozai mechanism (e.g., Wu & Murray 2003; Zakamska & Tremaine 2004; Takeda & Rasio 2005). The most popular mechanism to explain the eccentricity distribution is planet-planet interaction. This is not surprising because the Kozai mechanism requires a highly inclined companion, and hence cannot be applied to all the cases, while planet-disk interaction has to occur before planet-planet interaction, and therefore the eccentricity distribution achieved from the mechanism may be modified by planet-planet interaction after the gas disk dissipates. The previous studies have shown that planet-planet interaction can successfully reproduce the eccentricity distribution of extrasolar planets (e.g., Ford & Rasio

2007; Juric & Tremaine 2007; Chatterjee et al. 2007). However, these studies have also shown that the mechanism alone cannot explain the semi-major axis distribution if giant planets are formed beyond the ice line or even ~ 1 AU.

In this proceeding, we will investigate planet migration followed by planet-planet interaction as a scenario for explaining the current semi-major axis and eccentricity distributions of extrasolar planets. This kind of study has been done by many authors including Snellgrove et al. (2001); Lee & Peale (2002); Laughlin et al. (2002); Adams & Laughlin (2003); Moorhead & Adams (2005). Among these, Adams & Laughlin (2003); Moorhead & Adams (2005) are the most relevant work to us. They considered a model in which two planets exist in a cavity of a background gas disk. Since the planet closest to the gap edge feels the strongest torque in such a configuration, they applied a damping force only to the outer planet to mimic the differential migration. They also included the eccentricity damping due to the gas disk, relativistic corrections, as well as the tidal interactions with the central star, and reproduced the overall trend in the a-e distribution.

Our work follows their idea, but treats planet migration and disk evolution more self-consistently. We focus on the systems with three planets which are originally embedded in a gas disk. We will show that as the gas disk dissipates, the planetary systems become dynamically unstable. In §2, we will introduce the code we use to simulate such a system, and also summarize the initial conditions of the runs. In §3, we will show our results, focusing on a specific case and statistics. Finally in §4, we will discuss the results and summarize our work.

2. Numerical Methods and Initial Conditions

In this section, we first introduce the hybrid code we use to simulate the planetary systems with a dissipating gas disk. We also summarize the initial conditions used in the simulations.

2.1. A Hybrid SyMBA and 1D Gas Dynamics Code

For this study, we will use an existing N-body code which has added to it 1D gas dynamics (Thommes 2005) as well as gas accretion (Matsumura et al. 2008). The N-body part is based on a symplectic integrator `SyMBA` (Duncan et al. 1998), which combined the N-body map of Wisdom & Holman (1991) with an adaptive timestep to handle the close encounters. The gas disk is divided into radial bins with azimuthally and vertically averaged properties (e.g., surface mass density, viscosity, and temperature). The viscous evolution of a gas disk follows a standard α parameter prescription (Shakura & Sunyaev 1973), and the tidal interaction between planets and a disk is evaluated as in Menou & Goodman (2004) (also see Matsumura et al. 2007). The code also includes the eccentricity damping in a gas disk as in Papaloizou & Larwood (2000), as well as gas accretion onto a planet (Matsumura et al. 2008).

There are a few limits in the code which should be noted. First of all, the gas disk is one dimensional. This is potentially important since planet migration was observed to be slowed down in two or three dimensional disks (e.g., Tanaka et al. 2002; D'Angelo et al. 2003). However, the two or three dimensional effects are implicitly included by softening the tidal torque (Menou & Goodman 2004;

Matsumura et al. 2007). We adjusted the tidal torque until we had a reasonable agreement with Tanaka et al. (2002).

Secondly, the torque raised by planet-disk interaction does not include the corotation torque. Since the corotation torque is proportional to the gradient of the surface mass density relative to the disk's vorticity, it becomes important only when the surface mass density changes sharply — e.g., when the planet opens a gap. For example for Saturn-mass planets, it's been shown that planetary migration can be strongly affected by the corotation torque (e.g., Masset & Papaloizou 2003), but we don't take account of this effect in this work.

Thirdly, the temperature profile is fixed throughout the simulations. To better evaluate the viscous evolution of the disk, the radiative transfer should be included in the code.

2.2. Initial Conditions

Our goal is to find a set of initial conditions which could reproduce the observed eccentricity and semi-major axis distributions. The relevant parameters are planetary mass M, semi-major axis a, eccentricity e, inclination i, and the phase angles for planets, and surface mass density Σ and disk evaporation timescale $t_{\rm evap}$ for gas disks. For the planetary masses, we choose three planets randomly from the mass distribution of $d\log(M)/dN = 1$ from $M = 0.05 - 4\ M_J$. Ideally, planet formation should be simulated from the planetesimal size (or even smaller), but we will defer this to the future paper (Thommes et al. 2008, in preparation). The initial semi-major axis of the innermost planet is set to 5 AU. The other planets are located at 3.8 times the mutual hill radii from their nearest neighbors. The eccentricity, inclination and phase angles are randomly chosen from $e = 0 - 0.1$, $i = 1 - 10$ degrees, and $0 - 360$ degrees respectively. Since there are already massive planets at the start of the simulation, we will not use a primordial gas disk. Instead, the initial gas surface mass density is obtained by evolving the minimum mass solar nebula disk ($\Sigma = 10^3(a/AU)^{-3/2}$) for 7×10^6 years with the standard viscosity parameter of $\alpha = 5 \times 10^{-3}$. We also set the gas disk dissipation timescale. After this time is reached, a gas disk is exponentially removed, which mimics the rapid dispersal of gas disks seen in observations. We run 100 simulations each for the gas dissipation timescale of 1, 2, 3, and 4×10^6 years. The choice of gas dissipation timescale is motivated by the observed lifetime of protoplanetary disks ($10^6 - 10^7$ years) with respect to our initial disk age.

3. Results

In this section, we will show the results of our simulation. First, we show a typical example, and then show a statistical result out of a sample of 400 planetary systems.

3.1. A Typical Example

Before showing the statistical result, we will present an example case. Here, the planetary masses are 0.8, 1.2, and 1.8 Jupiter masses, and the inner most planet is initially located at 5 AU. All planets are separated by 3.8 times the mutual hill radii from their nearest neighbors. In this run, the disk is exponentially

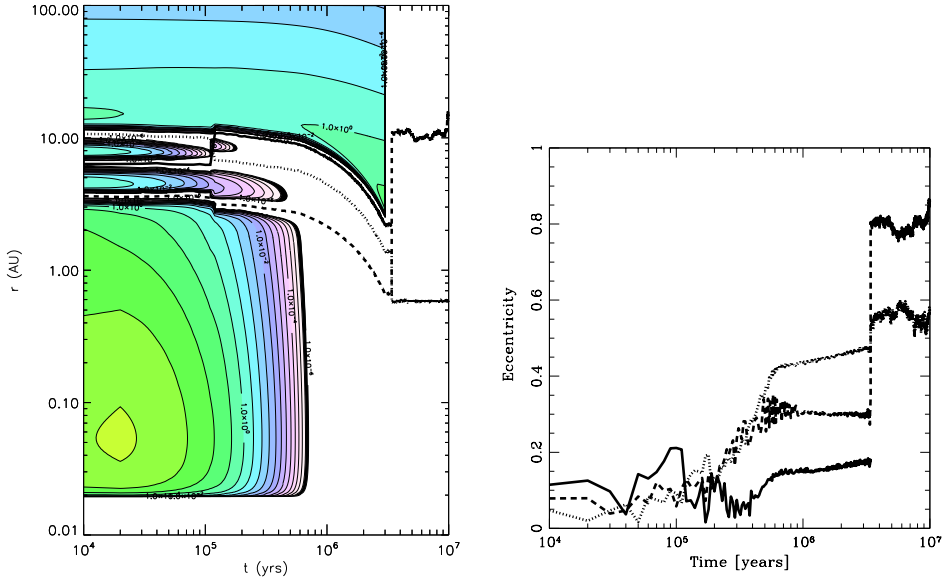

Figure 1. Left: Time evolution of semi-major axes of 3 planets. The contours are the surface mass density. The solid, dashed and dotted lines show the evolution of a planet with 1.2 M_J, 0.8 M_J, and 1.8 M_J respectively. Right: Time evolution of eccentricities of 3 planets. The 1.2 M_J planet gets ejected, leaving the other two planets in highly eccentric orbits (~ 0.8 for 0.8 M_J and ~ 0.6 for 1.8 M_J.

dissipated after 3 million years, which corresponds to the disk's lifetime of 10 million years since the initial disk is already evolved for 7 million years.

The left panel of Fig. 1 shows the disk evolution as well as the orbital evolution of planetary systems. All planets will remove the gas annuli between them by 0.5 million years, and the inner gas disk dissipates before 0.7 million years from the start of the simulation. An orbital crossing is seen before the disk dissipation around 10^5 years, but the major scattering events don't occur until the gas disk dissipates after 3 million years. Around 3.5 million years, the second most massive planet (the solid line) gets ejected out of the system.

The right panel of Fig. 1 shows the eccentricity evolution of the same run. The eccentricity is overall increasing throughout the simulation, with two characteristic jumps. The first jump in the eccentricity occurs at around 0.5-0.7 million years, corresponding to the dissipation of gas annuli between planets and the inner disk dissipation. The second jump in the eccentricity occurs just after the outer disk dissipation, and the ejection of the second most massive planet. The ejection of this planet leads to the orbital crossing and the higher eccentricities of the remaining planets.

3.2. Statistics

We perform 400 runs similar to the one shown in the previous subsection. We use different dissipation timescales for each set of 100 runs (1, 2, 3, and 4 million years). The final results are shown in Fig. 2.

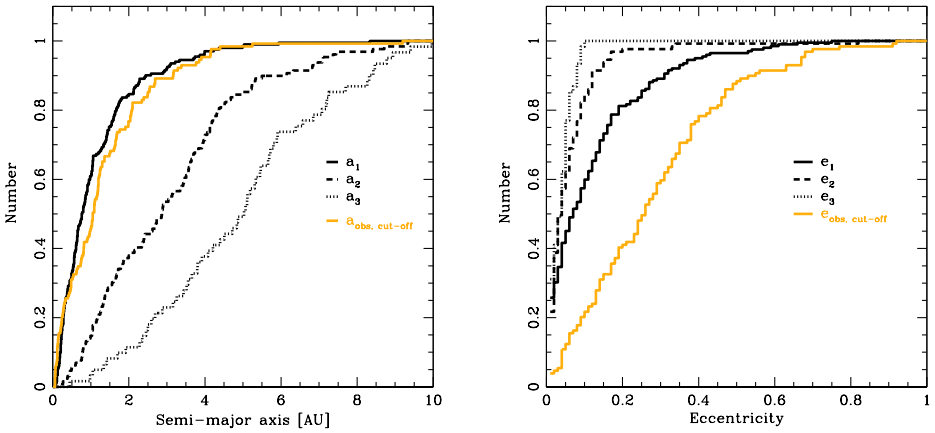

Figure 2. Left: Cumulative distributions of semi-major axis compared with the observed distribution. The subscripts $1-3$ correspond to the innermost, medium, and outermost planets at the end of the simulations (10^7 years). The distribution of the innermost planets shows a good agreement with the observed distribution. Right: Cumulative distributions of eccentricity compared with the observed distribution. The distribution of the innermost planets is the closest to the observed distribution, but they don't have a good agreement.

The left panel of Fig. 2 is the cumulative distribution of semi-major axis. The subscripts 1, 2, and 3 imply the innermost, middle, and outermost planets at the end of the simulations (10^7 years) respectively. It is clear that the innermost planet gives a reasonable agreement to the observed semi-major axis distribution. Here, the observed distribution includes the planets which have the mass of $M_p = 0.05 - 4.0 M_J$, and the semimajor axis of $a > 0.06$ AU. The planetary mass limit is applied because of our initial conditions, while the semimajor axis limit is applied because planets so close to the central star ($a \leq 0.06 AU$) are likely to suffer the effect of tidal circularization which we have not included in this study. The right panel of Fig. 2 is the corresponding cumulative distribution of eccentricity. We do not get as good agreement here as the semi-major axis. We have tried different initial conditions (e.g., randomly chosen mass or semi-major axis), but the agreement did not improve significantly.

By examining the eccentricity-semimajor axis plot, we have found that we overproduced planets with small eccentricity and large semi-major axis. This could imply that planets are formed in a more packed system, or in other words, the systems with three planets tend to be inactive when they emerge out of the gas disk. Juric & Tremaine (2007) showed that "Hill separation", which is the minimum distance between two planets' orbits normalized by their mutual Hill radii, could be used to distinguish active, partially active, and inactive systems. In our simulations, 80 out of 400 systems still keep all three planets just after gas disks are exponentially removed, while this number goes down to 53 by the end of the simulations. Therefore, 27 out of 80 systems go through dynamical instability characterized by ejections and mergers after the gas disk dissipation. Calculating Hill separations for these systems at the time of disk dissipation, we

find that 22 out of 27 indicate that they have at least one active/partially active pair of planets while the other systems are "inactive". On the other hand, 51 out of 53 systems which retain all three planets throughout the simulations also have at least one active/partially active pair of planets. This may imply that, with longer runs, some of these systems also go through dynamical instability. We have run the simulations up to 10^9 years, which is about the age of typical planet-hosting stars, but we did not find a significant improvement in semi-major axis distributions.

4. Summary

In this proceeding, we explore the initial conditions which could reproduce the semi-major axis and eccentricity distributions of extrasolar planetary systems. We simulate the evolution of systems with three planets by including gas disk dissipation, and compare the statistics out of 400 cases with the observed distributions. We find a relatively good agreement for the semi-major axis distribution, but not for the eccentricity distribution. From the eccentricity-semimajor axis plot, we deduced that our simulations tend to overproduce the planets with low eccentricity and large semimajor axis. From the median Hill separation, we found that this does not necessarily mean that three-planet systems are inactive when they emerge out of gas disks. We are currently investigating this problem further by using different surface mass densities, and larger number of planets.

Acknowledgments. This work was supported by NSF grant AST-0507727. E. W. T. and F. A. R. are supported in part by the Spitzer Space Telescope Cycle-4 Theoretical Research Program through Grant pid-40380.

References

Adams, F. C. & Laughlin, G. 2003, Icarus, 163, 290
Artymowicz, P. 1993, ApJ, 419, 166
Chatterjee, S., Ford, E. B., & Rasio, F. A. 2007, ArXiv Astrophysics e-prints
D'Angelo, G., Kley, W., & Henning, T. 2003, ApJ, 586, 540
Duncan, M. J., Levison, H. F., & Lee, M. H. 1998, AJ, 116, 2067
Ford, E. B. & Rasio, F. A. 2007, ArXiv Astrophysics e-prints
Goldreich, P. & Sari, R. 2003, ApJ, 585, 1024
Goldreich, P. & Tremaine, S. 1979, ApJ, 233, 857
Juric, M. & Tremaine, S. 2007, ArXiv Astrophysics e-prints
Laughlin, G., Chambers, J., & Fischer, D. 2002, ApJ, 579, 455
Lee, M. H. & Peale, S. J. 2002, ApJ, 567, 596
Lin, D. N. C. & Ida, S. 1997, ApJ, 477, 781
Masset, F. S. & Papaloizou, J. C. B. 2003, ApJ, 588, 494
Matsumura, S., Pudritz, R. E., & Thommes, E. W. 2007, ApJ, 660, 1609
—. 2008, in preparation
Menou, K. & Goodman, J. 2004, ApJ, 606, 520
Moorhead, A. V. & Adams, F. C. 2005, Icarus, 178, 517
Papaloizou, J. C. B. & Larwood, J. D. 2000, MNRAS, 315, 823
Rasio, F. A., Tout, C. A., Lubow, S. H., & Livio, M. 1996, ApJ, 470, 1187
Shakura, N. I. & Sunyaev, R. A. 1973, A&A, 24, 337
Snellgrove, M. D., Papaloizou, J. C. B., & Nelson, R. P. 2001, A&A, 374, 1092
Takeda, G. & Rasio, F. A. 2005, ApJ, 627, 1001
Tanaka, H., Takeuchi, T., & Ward, W. R. 2002, ApJ, 565, 1257

Thommes, E. W. 2005, ApJ, 626, 1033
Thommes, E. W., Matumura, S., & Rasio, F. A. 2008, in preparation
Ward, W. R. 1997, Icarus, 126, 261
Weidenschilling, S. J. & Marzari, F. 1996, Nature, 384, 619
Wisdom, J. & Holman, M. 1991, AJ, 102, 1528
Wu, Y. & Murray, N. 2003, ApJ, 589, 605
Zakamska, N. L. & Tremaine, S. 2004, AJ, 128, 869